

1 USE OF WASTE-DERIVED BIOCHAR TO REMOVE COPPER FROM AQUEOUS  
2 SOLUTION IN A CONTINUOUS-FLOW SYSTEM

3

4 Diego Arán<sup>a,b</sup>, Juan Antelo<sup>b,\*</sup>, Pablo Lodeiro<sup>c</sup>, Felipe Macías<sup>a</sup>, Sarah Fiol<sup>b,d</sup>

5

6 <sup>a</sup>Department of Soil Science and Agricultural Chemistry, University of Santiago de  
7 Compostela, 15782 Santiago de Compostela, Spain

8 <sup>b</sup>Instituto de Investigaciones Tecnológicas, University of Santiago de Compostela,  
9 15782 Santiago de Compostela, Spain

10 <sup>c</sup>Department of Chemical Oceanography, GEOMAR – Helmholtz Centre for Ocean  
11 Research Kiel, 24148 Kiel, Germany

12 <sup>d</sup>Department of Physical Chemistry, University of Santiago de Compostela, 15782  
13 Santiago de Compostela, Spain

14 \*Corresponding author. E-mail: [juan.antelo@usc.es](mailto:juan.antelo@usc.es)

1 **Abstract**

2 The discharges from industrial processes constitute the main source of copper  
3 contamination in aqueous ecosystems. In this study we investigated the capacity of  
4 different types of biochar (derived from chicken manure, eucalyptus, corncob, olive mill  
5 and pine sawdust) to remove copper from aqueous solution in a continuous-flow  
6 system. The flow rate of the system strongly influenced the amount of copper retained.  
7 The adsorption to the corncob biochar varied from 5.51 to 3.48 mg Cu g<sup>-1</sup> as the flux  
8 decreased from 13 to 2.5 mL min<sup>-1</sup>. The physicochemical characteristics of biochar  
9 determine the copper retention capacity and the underlying immobilization mechanisms.  
10 Biochars with high inorganic contents retain the largest amounts of copper and may be  
11 suitable for using in water treatment systems to remove heavy metals. The copper  
12 retention capacity of the biochars ranged between ~1.3 and 26 mg g<sup>-1</sup> and varied in the  
13 following order: chicken manure > olive mill >> corncob > eucalyptus > sawdust pine.

14

15 **Keywords:** Sorption, Biochar, Copper, Slow pyrolysis, Continuous-flow systems

## 1 **1. Introduction**

2 Increased industrialization during the last century has had a substantial impact on the  
3 environment due to the accumulation of heavy metals in soils and sediments. These  
4 heavy metals are persistent, non-biodegradable and show high toxicity, affecting flora  
5 and fauna of the ecosystems. Copper is one of the most widely used metals as it is  
6 required in many industrial processes (metallurgy, power generation and transmission,  
7 electronic manufacturing, mining and agriculture). The waste produced during these  
8 processes constitutes the main source of copper and other metals in soils and water.<sup>1</sup>  
9 The harmful effects of such contaminants have driven the development of remediation  
10 methods based on chemical precipitation, adsorption/co-precipitation on metal oxides,  
11 ionic exchange and filtration. However, some treatments require expensive reagents  
12 and/or equipment and may also generate huge amounts of waste.<sup>2</sup>

13 The increasing use of inexpensive materials to remove pollutants from the environment  
14 has prompted an interest in carrying out adsorption studies. The main goal of these  
15 adsorption studies is to test different types of material with a view to extrapolating the  
16 results to larger scale application. Among the different types of biomass tested for their  
17 capacity to scavenge heavy metals, algae and fungi have gained attention because of  
18 their elevated retention capacities as well as their wide availability and affordability.<sup>3,4</sup>  
19 The use of biochar (BC) as an adsorbent material also represents an inexpensive option  
20 for the efficient removal of contaminants from waste water. Biochar is a low-density  
21 carbonized material obtained by the combustion of biomass under conditions of low  
22 oxygen atmosphere and low temperature.<sup>5</sup> Various types of plant and animal-derived  
23 waste have been used to produce BCs in recent years.<sup>6,7</sup> Different studies have  
24 demonstrated the ability of BCs to remove Pb, Cu, Zn, Ni and Cr from aqueous  
25 solutions.<sup>8-10</sup> Biochar is considered suitable for restoring heavily contaminated

1 environments, such as areas affected by acid mine drainage, because of its high capacity  
2 to retain metals.<sup>11</sup> The high retention capacity is due to the affinity of BC for metal  
3 species and to changes in the chemical and physical properties of soil in relation to pH,  
4 electric conductivity and cationic exchange capacity. The retention capacity of BC can  
5 be due to (i) electrostatic interactions, (ii) ionic exchange, and (iii) sorption by p  
6 electrons delocalized from carbon.<sup>12</sup> Alternative immobilization mechanisms may  
7 involve precipitation and complexation.<sup>6,9</sup> Most studies that assess the ability of  
8 adsorbent materials to retain contaminants are based on batch experiments. However,  
9 the performance of these bioadsorbents should also be assessed in continuous systems  
10 to provide a more accurate picture of how they act in real situations, e.g. for  
11 decontaminating water.<sup>13,14</sup>

12 Continuous-flow experiments carried out using adsorption columns have provided  
13 useful information in addition to that obtained in batch adsorption experiments.<sup>15,16</sup>  
14 Ramírez-Pérez et al.<sup>17</sup> performed column experiments to assess the ability of mussel  
15 shell amendments to retain heavy metals from a mine soil. These authors concluded that  
16 the addition of this waste material to the soil increased the retention capacity and the pH  
17 of the soil and decreased the potential desorption of heavy metals. The effects of the  
18 physical and chemical properties of the column influent must be established in addition  
19 to the optimal operational parameters in order to increase the efficiency of the adsorbent  
20 materials. For example, an increase in the ionic concentration and pH of the influent  
21 solution led to the removal of more copper from solution when activated carbon was  
22 used in fixed-bed columns.<sup>18</sup> Fixed-bed column experiments with an alkali-modified  
23 biochar derived from hickory wood showed good immobilization of heavy metals (Pb,  
24 Cd, Cu, Zn, Ni) from aqueous solution, and regeneration of the column was possible  
25 after washing with acid solution.<sup>19</sup>

1 The main of the present study was to assess the performance of different types of BC to  
2 remove copper from an aqueous solution in continuous-flow adsorption columns. For  
3 this purpose, BCs were produced by pyrolysis of different types of feedstock material at  
4 low temperature. The specific objectives of the study were (i) to determine the influence  
5 of the flow rate on the efficiency of the biochar to remove copper in a continuous flow  
6 system, (ii) to determine and compare the capacity of the different types of biochar to  
7 retain copper from aqueous solution, and (iii) to determine the relationships between the  
8 characteristics of the different types of BC and their copper retention capacity.

## 9 **2. Materials and Methods**

### 10 2.1. Preparation and characterization of the biochar samples

11 Biochars were produced from different types of waste material: chicken manure  
12 (CMBC), eucalyptus (EBC), corncob (CCBC), olive mill waste (OBC) and pine  
13 sawdust (SBC). The details of the pyrolysis process for CMBC, EBC, CCBC and OBC,  
14 as well as the physical treatments applied to the different BCs are described in a  
15 previously published paper.<sup>9</sup> Briefly, the BCs were produced by slow pyrolysis at 300°C  
16 for 4 h under oxygen-limited conditions.

17 Total C, H, N and S contents were determined in an element analyzer (TruSpec CHN-  
18 1000, LecoSC-144DR). The ash content was determined by combustion of samples at  
19 1000 °C for 6 h in muffle furnace (C.H.E. S.A. HT BT S7 RP 1200 °C). The O content  
20 was determined as follows:  $O (\%) = 100 - (C\% + H\% + N\% + S\% + Ash\%)$ . The  
21 surface area ( $S_{BET}$ ) was determined by  $N_2$  adsorption with a Micromeritics Gemini 2360  
22 V2.01 instrument. The physicochemical characteristics of the different types of BC are  
23 summarized in Table 1.

## 1 2.2. Fixed-bed column experiments

2 The continuous flow adsorption experiments were conducted in a glass column, of 15  
3 mm internal diameter and 40 cm length, filled with 5 g of BC. The BC samples were  
4 packed in the columns as follows (Figure 1). First, a layer of glass wool was packed in  
5 the bottom of the column, to support the fixed bed. A 5 cm layer of acid-cleaned quartz  
6 sand (0.5–0.6 mm average particle size) was then placed on top of the glass wool. The  
7 central part of the column was packed with the BC samples (1–2 mm average particle  
8 size) to form a layer of thickness 9 cm. The BC particle size was selected to avoid  
9 clogging problems and high-pressures inside the column systems, which particles <0.5–  
10 1 cm may cause.<sup>20</sup> Finally, a layer (10 cm thick) of acid-cleaned quartz sand was packed  
11 in the top of the column to prevent loss of biomass and to ensure that all of the material  
12 was tightly packed. The column was washed with double distilled water for 0.5 h, and a  
13 copper solution ( $5 \text{ mg}\cdot\text{L}^{-1}$ ) (prepared from a  $\text{Cu}(\text{NO}_3)_2\cdot 3\text{H}_2\text{O}$  salt, Merck) was then fed  
14 through the column at different flow rates by a peristaltic pump (Masterflex) connected  
15 to the bottom end of the column and operating in up-flow mode. The pH of the copper  
16 influent solution was adjusted to  $5.0 \pm 0.1$  in all experiments by addition of small  
17 aliquots of 0.1 M NaOH or  $\text{HNO}_3$  solutions.

18 Several experiments were conducted at different flow rates (2.5, 5.0, 7.0 and 13.0 mL  
19  $\text{min}^{-1}$ ), with CCBC as the sorbent material, to evaluate the effect of the flow rate on the  
20 removal of copper from aqueous solution. Subsequent continuous-flow experiments  
21 were then carried out at a constant flow rate of  $7.0 \text{ mL min}^{-1}$ , to compare the capacity of  
22 the different types of BC to remove copper from the solution. Aliquots of the effluent  
23 were collected periodically with an autosampler, and the concentration of copper was  
24 determined by atomic absorption spectroscopy (AAS, Perkin Elmer 1100B). For

1 selected experiments, the concentration of free copper in the effluent was determined by  
2 ion selective electrode (ISE) potentiometry with an ELIT 8227 crystal membrane  
3 electrode. Finally, the pH of the samples collected was measured with Radiometer  
4 GK2401C pH electrode (Ag/AgCl reference). All experiments were performed in  
5 duplicate, at room temperature. Average values and the corresponding standard  
6 deviations were calculated for the exact replicates.

### 7 2.3. Analysis of column data

#### 8 2.3.1. Mathematical analysis

9 Copper retention in BC columns was assessed by examination of breakthrough curves,  
10 which show the shape of the concentration profile, expressed as the ratio between the  
11 concentration of copper in the effluent and in the influent ( $C/C_0$ ) over time. Numerical  
12 integration of the breakthrough curves provides several useful parameters, including the  
13 total amount of copper retained by the column,  $q_{total}$  (mg), which is expressed by the  
14 following equation:

$$q_{total} = \left( \frac{F}{1000} \right) \int_{t=0}^{t=t} C_{ads} dt \quad (1)$$

15 where  $C_{ads}$  ( $\text{mg L}^{-1}$ ) is the difference between the initial concentration of copper in the  
16 influent ( $C_0$ ) and the concentration in the effluent ( $C$ ) at any time;  $t$  (min) is the time  
17 during which the solution sample circulates through the column, and  $F$  ( $\text{mL min}^{-1}$ ) is the  
18 flow rate. The amount of copper retained in equilibrium ( $q_e$ ), expressed in  $\text{mg g}^{-1}$ , can  
19 be calculated as  $q_e = q_{total}/M$ , where  $M$  (g) is the amount of adsorbent material in the  
20 column. Other important parameters used to describe the breakthrough curves include  
21 the breakthrough point ( $t_b$ ), which is usually defined as the time needed for the  $C/C_0$   
22 ratio in the effluent to decrease to a value of 0.5 (i.e. so that only 50% of the sorbate

1 remains in the outflowing solution). However, the limiting value of  $C/C_0$  can be  
2 established at different values, depending on the purpose and aims of the study and any  
3 further applications intended for the effluent. Thus, reductions in the initial  
4 concentration of between 3 and 5% have been used by Chen et al.<sup>18</sup> to study copper  
5 retention by activated carbon. On the other hand, Lodeiro et al.<sup>3</sup> established an even  
6 lower value for this ratio, based on European directives, and recommended specific  
7 limits for dissolved Cd in water from industrial effluents. In the present study, the  $C/C_0$   
8 ratio was established as 0.05, which is equivalent to 0.25 mg L<sup>-1</sup> of copper in the  
9 effluent. This value corresponds to the limit for wastewater discharges established by  
10 the BSR (Business for Social Responsibility) Water Quality Guidelines.<sup>21</sup> This limit is  
11 quite strict in view of the range of existing limits in international legislation, which vary  
12 from 0.5 to 3 mg L<sup>-1</sup> for waste water discharges<sup>22, 23</sup>, and from 0.05 to 2 mg L<sup>-1</sup> for  
13 water destined for human consumption or for irrigation.<sup>24-26</sup> Additional parameters  
14 include the exhaustion time ( $t_e$ ), defined as the time when the ratio  $C/C_0$  reaches a value  
15 of 0.95, and the length of the mass transference front ( $Z_m$ ), which can be derived from  
16 the following equation:

$$Z_m = Z \left(1 - \frac{t_b}{t_e}\right) \quad (2)$$

17 where  $Z$  is the length of the column, in cm, and the time interval between  $t_b$  and  $t_e$  ( $\Delta t$ ),  
18 known as adsorption zone, is indicative of the rate of mass transfer.

### 19 2.3.2. Modelling the breakthrough curves

20 A non-linear equation based on the Bohart-Adams model<sup>27</sup> was used to fit the  
21 breakthrough curves obtained from the column experiments. The Bohart-Adams model  
22 can be used for systems in which the equilibrium is highly favorable. This model  
23 assumes that the surface reaction is the rate-limiting step, and uses an irreversible



1 (rectangular) sorption isotherm to describe equilibrium. Despite the premises of its  
2 derivation and of its simplicity, the Bohart-Adams model is able to reproduce the  
3 experimental breakthrough curves and has been widely used to describe fixed bed  
4 continuous-flow systems and to calculate the maximum adsorption capacity of  
5 adsorbents.<sup>28,29</sup> Moreover, fitting data to the Bohart-Adams model generally results in  
6 lower errors than using its mathematically equivalent Thomas model<sup>30</sup>, especially for  
7 times far from the breakthrough point. The expression proposed by Yan et al.<sup>27</sup> for the  
8 modified Bohart-Adams model, which is based on statistical analysis of experimental  
9 data, was used in the present study and is expressed as follows:

$$C/C_0 = 1 - \frac{1}{1 + \left( \frac{C_0 * F}{q_{max} * M} * t \right)^a} \quad (3)$$

10 where  $a$  is an empirical parameter related to the slope of the regression function and  
11  $q_{max}$  is the maximum adsorption capacity of the BC ( $\text{mg g}^{-1}$ ). Both parameters,  $q_{max}$  and  
12  $a$ , were used as fitting parameters. The models derived from the Bohart-Adams model  
13 were only used to describe the experimental breakthrough curves, regardless of  
14 theoretical considerations, and to detect any correlations between the model parameters  
15 and the experimental variables.

### 16 **3. Results and Discussion**

#### 17 **3.1. Characterization of the biochar samples**

18 The different BC samples were classified according to their C contents, as follows: high  
19 C content (85.2%), CCBC; intermediate C content (69.3 and 62.6%), EBC and SBC,  
20 and low C content (32.6 and 31.1 %), CMBC and OBC. The C content was lowest in  
21 the BCs with the highest inorganic contents, i.e. with more than 45% ash (Table 1). The  
22 inorganic fraction of these biochars was previously characterized by X-ray

1 diffractometry (XRD) and the main mineral components identified in CMBC and OBC  
2 were quartz ( $\text{SiO}_2$ ), calcite ( $\text{CaCO}_3$ ) and struvite ( $\text{MgNH}_4\text{PO}_4 \cdot 6\text{H}_2\text{O}$ ).<sup>9</sup> The N content  
3 varied between 0.41 % and 3.02 %, and the S content between 0.01 % and 0.32 %. The  
4 N contents were much higher in the BCs with the lowest C contents, as reported by  
5 Ahmad et al.<sup>31</sup>, who attributed this finding (which is also applicable to S) to the type of  
6 feedstock material used to produce the BC rather than to the pyrolysis conditions.

7 The degree of carbonization and condensation of aromatic rings can be described on the  
8 basis of the H/C molar ratio. Low H/C ratios indicate a high degree of aromatization  
9 and good stability. Conversely, high H/C ratios are indicative of materials that are  
10 scarcely transformed by pyrolysis or that have low contents of lignocellulosic  
11 compounds. H/C ratio has been reported as a smart linkage between BC characteristics  
12 and pyrolytic temperatures.<sup>32</sup> Xiao et al.<sup>32</sup> obtained a quantitative relationship between  
13 pyrolysis temperature and H/C atomic ratio for a wide range of BC despite the great  
14 variety of precursor feedstock. This relationship showed a decrease in H/C, that is, an  
15 increase in aromaticity, with the heating temperature. The H/C ratio of the BCs studied  
16 here varied between 0.29 and 1.45 (Table 1). These values are within the range reported  
17 by Xiao et al.<sup>32</sup> for BC obtained at a pyrolysis temperature around 300 °C. Values  
18 within a similar range and pyrolysis temperature have been also reported by other  
19 authors: 0.67 for BCs derived from peanut shells<sup>33</sup>, 0.52 for a BC derived from  
20 hardwood<sup>34</sup> or 0.75 for a pine needles derived BC. The O/C molar ratio of the BCs  
21 varied between 0.07 and 0.37 (Table 1). High polarity (due to the presence of abundant  
22 oxygenated functional groups) leads to high O/C ratios ( $>0.25$ ), such as those obtained  
23 for SBC, CMBC and OBC. On the other hand, O/C ratios  $\leq 0.25$ , such as those obtained  
24 for CCBC and EBC, are indicative of low polarity. Intermediate O/C values similar to  
25 those obtained for most of the samples of the present study ranged between 0.27 and

1 0.29 for plant-derived BCs at the same pyrolysis temperature<sup>33-35</sup>. O/C values in the  
2 range 0.1-0.63 have been reported for BCs elaborated from pine needles, the lowest  
3 value corresponding to BC produced by pyrolysis of the material at high temperature  
4 (600 °C) and the highest value for the BC produced by pyrolysis at a lower temperature  
5 (100 °C).<sup>35</sup> Lower O/C values, in the range 0.06-0.107, have been reported for BC  
6 derived from wheat residue combusted at different pyrolysis temperatures.<sup>36</sup> The Van  
7 Krevelen diagram for the different types of BC in the present study showed that the  
8 values of both ratios (H/C and O/C) were within the range of values reported for  
9 different types of biochar, derived from plants, animal material or residues such as  
10 sewage sludge (Figure S1).

11 The specific surface area ( $S_{BET}$ ) data provided a very heterogeneous set of values for the  
12 different types of BC (Table 1), ranging from 1.60 m<sup>2</sup> g<sup>-1</sup> for EBC to 173 m<sup>2</sup> g<sup>-1</sup> for  
13 CCBC. The surface area of BC is affected by the nature of the feedstock material and  
14 also by pyrolysis conditions, with higher temperatures yielding larger surface areas.  
15 Moreover, pre-treatment with NaOH or KOH facilitates opening and cleaning of the  
16 pores, thus also producing a larger surface area.<sup>19,36</sup>

### 17 3.2. Effect of flow rate on the optimization of working conditions of the columns

18 The copper breakthrough curves obtained for the CCBC fixed-bed column at the  
19 different flow rates are shown in Fig. 2. An increase in the inflow rate caused a decrease  
20 in the saturation time. The parameters derived from the experimental data plotted in the  
21 breakthrough curves (Table 2) revealed different relationships with the operational flow  
22 rate. Integration of the breakthrough curves for copper adsorption on CCBC led to an  
23 increase in  $q_{total}$  and  $Z_m$  as the flow rate was increased up to 7.0 mL min<sup>-1</sup>. Nevertheless,  
24 no further increase was observed in  $q_{total}$  between 7.0 and 13.0 mL min<sup>-1</sup>, which is

1 consistent with the almost coincident breakthrough curves obtained at both flow rates  
2 (Figure 2). Analysis of breakthrough time,  $t_b$ , and saturation time,  $t_e$ , plotted against the  
3 flow rate revealed inverse linear correlations within the interval 2.5-7.0 mL min<sup>-1</sup>. Less  
4 variation was observed in these two parameters for the interval 7.0-13 mL min<sup>-1</sup> (Figure  
5 3). This finding can be explained by considering that an increase in the flow rate beyond  
6 a certain value will reduce the residence time of the solution in the column, thus  
7 preventing the solution from reaching the interior of the pores and causing the  
8 appearance of the solute in the effluent before the adsorption equilibrium is reached.  
9 This effect has been reported for copper and other contaminants at high flow rates.<sup>37,38</sup>  
10 The reduction in the flow rate resulted in less steep breakthrough curves (Figure 2) as a  
11 consequence of the longer breakthrough and saturation times required for complete  
12 exhaustion of the column (Table 2). Parameter  $\Delta t$  was strongly and negatively  
13 correlated ( $R=-0.999$ ) with the flow rate, leading to an increase in the transference zone  
14 as the flow rate increases. Taking these results into account, the optimal operational  
15 flow rate of the fixed-bed columns was 7.0 mL min<sup>-1</sup>, and this rate was used in  
16 subsequent experiments carried out to investigate the capacity of the different types of  
17 BC to remove copper from aqueous solution.

18 The modified Bohart-Adams model provided acceptable fits for the experimental data  
19 obtained at the different flow rates, with correlations  $> 0.980$  and squared sum of  
20 residuals  $< 0.11$  (Figure 2). The fitting parameters are listed in Table 3. The  $q_{\max}$  value  
21 increased linearly with the flow rate ( $R^2 > 0.737$ ). The highest  $q_{\max}$  value, 5.51 mg g<sup>-1</sup>,  
22 was obtained for a flow rate of 13 mL min<sup>-1</sup>, and the lowest value, 3.48 mg g<sup>-1</sup>,  
23 corresponded to a flow rate of 2.5 mL min<sup>-1</sup>. The fitting parameter  $a$ , which is related to  
24 the slope of the regression, varied between 3.2 and 6.7. The decrease in parameter  $a$   
25 with the increase in flow rate was also linear ( $R^2 = 0.978$ ).

### 1 3.3. Comparison of copper sorption on different types of biochar

2 The copper breakthrough curves obtained with the BC samples under study are shown  
3 in Figure 4, and the parameters derived from these curves are shown in Table 4. All  
4 experiments were conducted at the same flow rate ( $7.0 \text{ mL min}^{-1}$ ) and with a fixed bed  
5 height of the adsorbent layer (9 cm). The copper concentration in the effluent did not  
6 quantitatively change between the AAS and ISE measurements. The breakthrough  
7 curves show that the BCs can be classified in two groups, with respectively a high and  
8 low capacity to remove copper from solution. The BCs with the highest copper  
9 retention capacities (CMBC and OBC) corresponded to those with the highest  $q_e$  and  $t_b$   
10 values, and the BCs with the lowest copper retention capacities (CCBC, EBC, SBC)  
11 were those with low  $q_e$  and  $t_b$  values (Table 4). There was no significant difference in  
12 the breakthrough time,  $t_b$ , obtained for CMBC and OBC, approximately 45 h. The  
13 breakthrough times for the other three samples were all below 10 h. The difference  
14 between breakthrough and saturation time,  $\Delta t$ , which is related to the rate of mass  
15 transfer, is consistent with the previous classification. The samples with the longest  
16 transfer intervals, CMBC and OBC, produced breakthrough curves with smoother  
17 slopes, whereas the slopes for CCBC, EBC and SBC, with shorter transfer intervals,  
18 were steeper. Smoother slopes indicate that saturation of the biochar material in the  
19 column takes longer. Curves with steeper slopes and short breakthrough times indicate  
20 that the retention capacity of the material is relatively low.

21 The initial effluents of the column filled with the sample EBC were yellow-brown  
22 coloured, pointing out to the presence of dissolved organic carbon (DOC). The content  
23 of soluble organic matter may affect the sorption capacity of the biochar. In a previous  
24 study, the DOC released from the sample EBC and its contribution to the binding of Cu  
25 was measured in batch experiments, accounting for  $\sim 18 \text{ mg C/L}$  and 75.7% of the Cu

1 bound, respectively.<sup>9</sup> Although DOC was not measured in the column effluents, the  
2 results obtained by AAS and ISE showed no significant differences in the amount of  
3 copper in solution thus meaning that all the Cu was sorbed in the biochar material  
4 within the column and not bound to the DOC released (see discussion in Aran et al.<sup>9</sup>).

5 Some of the parameters defined by the breakthrough curves were correlated with the  
6 physicochemical characteristics of the BCs. In previous batch studies of copper  
7 retention on BC, some physicochemical characteristics (i.e. pH, O/C ratio and ash, P  
8 and C content) were found to affect the amount of copper retained.<sup>9</sup> The pH of the  
9 effluent was measured as the copper containing solution went through the column. For  
10 those BC samples with  $\text{pH} \leq 7$  there was no difference between the initial pH of the  
11 solution entering the column and the effluent, whereas for the alkaline BC samples, e.g.  
12 OBC and CCBC, the pH decreased in the effluent during the working time of the  
13 column. In these cases, a steady pH value of 6.5 was reached after 4 h (Figure S2).

14 Copper is known to precipitate in slightly acidic to alkaline conditions as oxide,  
15 hydroxide or carbonate mineral forms. In the present study, Visual MINTEQ 3.1 was  
16 used to calculate the saturation indices and the formation of copper mineral phases  
17 under the experimental conditions.<sup>39</sup> Results revealed that the formation of tenorite  
18 (CuO) is favoured in the OBC and CCBC columns (Figure S3). Since the variation in  
19 the pH is comparable in both alkaline BCs, the difference observed for the retention  
20 capacity in these samples arises from their different chemical composition. According  
21 to this result, the mechanism of retention was found to differ depending on the amount  
22 of the inorganic and organic fractions, i.e. the predominance of the mineral fraction over  
23 the organic fraction resulted in higher retention capacities due to the combination of  
24 adsorption and precipitation processes. In the present study, copper retention was  
25 highest in samples with an O/C molar ratio higher than 0.3 and high ash and phosphorus

1 contents, above 40% and 3 g PO<sub>4</sub> kg<sup>-1</sup>, respectively (Table 1). As indicated by Xu et  
2 al.<sup>40</sup>, the formation of metal carbonates and phosphate precipitates is favored in mineral-  
3 rich biochars. Uchimiya et al.<sup>41</sup>, also indicated that heavy metals retention by biochar is  
4 enhanced in low carbonized biochar materials. Peng et al.<sup>42</sup> observed an enhancement in  
5 heavy metals retention on phosphoric modified BCs in comparison with the pristine BC  
6 due to the formation of additional complexes between functional groups, such as P=O  
7 and P=OOH, and the metal ions. In our previous study<sup>9</sup>, higher sorption of metals in  
8 batch experiments for mineral-rich biochars was explained by their higher cation  
9 exchange capacity and the precipitation of Cu<sub>3</sub>(PO<sub>4</sub>)<sub>2</sub>. Equilibrium concentration of PO<sub>4</sub>  
10 in distilled water was quantified for the sample OBC using a 1:10 solid:solution ratio.<sup>43</sup>  
11 This value was thereafter used to calculate the saturation indices for different copper  
12 phosphate mineral phases with Visual MINTEQ 3.1. These calculations revealed that  
13 formation of these compounds is possible under the experimental conditions of the  
14 fixed-bed column sorption experiment at pH values above 5.5 (Figure S3). According to  
15 the physicochemical characteristics of sample CMBC, circumneutral pH and high  
16 concentration of total phosphate, the immobilization mechanism for copper is expected  
17 to be similar to that of the OBC. Similar correlations between physicochemical  
18 properties and retention capacity were observed for other metals such as lead, zinc and  
19 cadmium, and the retention capacity was highest in BCs with the highest ash contents,  
20 i.e. in which the mineral fraction predominates.<sup>6,40</sup> In the present study, the  
21 physicochemical properties that were most closely correlated with the parameters of the  
22 breakthrough curves ( $q_e$ ,  $t_b$ ,  $t_e$ ) were %C, %N and %ash (Table S1). The highest positive  
23 correlation was found with the %ash, e.g. copper retention was favourable in the BCs  
24 with the highest inorganic contents, which is consistent with the results of batch

1 experiments.<sup>9</sup> As expected, the parameters of the breakthrough curves were negatively  
2 correlated with the %C.

3 The modified Bohart-Adams model fitted well to the experimental data (Figure 4),  
4 yielding  $R^2$  values higher than 0.970 and RRSE lower than 0.10 (Table 5). The  $q_{max}$   
5 values obtained for the different BC materials, i.e. the maximum retention capacity,  
6 varied as follow: CMBC > OBC > EBC > CCBC > SBC. The samples with the highest  
7 inorganic content, CMBC and OBC, retained more copper: 26.63 and 25.30 mg g<sup>-1</sup>,  
8 respectively. As expected, this parameter was closely correlated with the ash content ( $R^2$   
9 = 0.980). The BC with high organic content, reflected in higher %C and lower ash  
10 content, retained less copper, with a decrease in the  $q_{max}$  values ranging from 79 to 95 %  
11 (Table 5). Parameter  $a$ , obtained by fitting the modified Bohart-Adams model to the  
12 data, was not correlated with the physicochemical properties of the BCs. The values of  
13 this parameter ranged between 0.66 for SBC and 9.12 for OBC (Table 5).

14 The affinity sequence is consistent with the maximum adsorption capacity obtained in  
15 batch experiments conducted with the same BCs.<sup>9</sup> A good correlation was observed  
16 between the maximum adsorption capacities obtained with the Langmuir-Freundlich  
17 model (batch experiments) and those obtained with the modified Bohart-Adams model  
18 (continuous experiments) (Figure 5). The maximum retention capacity predicted by the  
19 modified Bohart-Adams model was also closely correlated with the breakthrough time  
20 ( $t_b$ ) ( $R^2=0.991$ ) (Figure S4). The good correlations between parameters enable direct  
21 prediction of the behavior of a given biochar in continuous systems and also enable the  
22 operational conditions of the columns to be established using the available information  
23 obtained in batch experiments.



1 The copper retention capacity of the BCs were similar to or higher than observed for  
2 other BCs. Biochar or activated carbon derived from different types of plant-waste such  
3 as pine, pomegranate wood, silver birch, jarrah and wheat straw had similar Cu  
4 retention capacities, of between 0.129 and 17.83 mg g<sup>-1</sup>.<sup>18,44-47</sup> Biochar materials derived  
5 from plant residues usually contain limited mineral components, but those derived from  
6 animal residues generally present higher mineral content and larger sorption capacities;  
7 e.g. swine manure and dairy manure biochars showed maximum sorption capacities of  
8 20.11 and 35.2 mg g<sup>-1</sup>, respectively.<sup>6,48</sup> Among the biochars used in the present study,  
9 CMBC and OBC appear to be the most suitable types of BC for copper retention,  
10 because they can remove higher amounts of Cu from aqueous solution and also because  
11 the removal mechanism involves co-precipitation and adsorption, thus producing more  
12 stable forms. The plant-derived biochars EBC, SBC and CCBC showed lower  
13 efficiency for the removal of copper from aqueous solution, which is partially caused by  
14 their lower content of mineral components. Further studies are needed to develop  
15 economical and suitable strategies for simultaneous metal sorption, regeneration  
16 methods and potential applications for the metal-loaded biochar materials.

#### 17 **4. Conclusions**

18 Flow rate is a key parameter in continuous flow systems with a high adsorption  
19 capacity. In the present study, high flow rates (> 7 mL min<sup>-1</sup>) yielded short  
20 breakthrough and saturation times, whereas intermediate to low flow rates provided  
21 optimal conditions for retention of copper by BC. Columns filled with CCBC and  
22 operating at flow rates of 7 and 5 mL min<sup>-1</sup> yielded breakthrough times of 5 and 12  
23 hours and maximum copper retention capacities of 3.78 and 4.55 mg g<sup>-1</sup>, respectively.

1 The copper retention capacities of the different types of BC tested in the present study  
2 were high, with values ranging from 1.28 mg g<sup>-1</sup> for SBC to 26.63 mg g<sup>-1</sup> for CMBC.  
3 Biochars may therefore be effective and economic alternatives to other sorbent  
4 materials for removing heavy metals from aqueous systems. The physicochemical  
5 characteristics of the materials used to produce the BCs determine the copper retention  
6 capacity and the underlying immobilization mechanisms. The biochars with the highest  
7 retention capacity, CMBC and OBC, were also those containing the highest amounts of  
8 inorganic compounds. These biochars may be suitable for use in water treatment  
9 systems to remove copper or other heavy metals. Finally, a good correlation was  
10 observed between the sorption parameters in continuous flow systems and in  
11 discontinuous systems. This enables prediction of the behaviour of BC materials and  
12 optimization of the operational conditions with very few sorption experiments.

### 13 **Acknowledgements**

14 The authors belong to the CRETUS Strategic Partnership (AGRUP2015/02), co-funded  
15 by FEDER (UE). This work was partially funded by the program Group of Excellence  
16 GI-1245 (GRC2014/003) and by the INTERREG V-A POCTEP Program  
17 (0366/RES2VALHUM/1/P). The authors are grateful to Alvaro Gil from the Ceramic  
18 Institute of the USC for the BET measurements, David Romero of the Department of  
19 Soil Science and Agricultural Chemistry for assistance in the AAS measurements, and  
20 the *Centro de Valorización Ambiental del Norte* (Touro, Spain) for preparing the  
21 biochar samples.

22

## 1 5. References

- 2 (1) Bogusz, A.; Oleszczuk, P.; Dobrowolski, R. Application of Laboratory Prepared and  
3 Commercially Available Biochars to Adsorption of Cadmium, Copper and Zinc Ions  
4 from Water. *Bioresour. Technol.* **2015**, *196*, 540–549. DOI:  
5 10.1016/j.biortech.2015.08.006
- 6 (2) Regmi, P.; García-MoscOSO, J.L.; Kumar, S.; Cao, X.; Mao, J.; Schafran, G.  
7 Removal of Copper and Cadmium from Aqueous Solution Using Switchgrass Biochar  
8 Produced via Hydrothermal Carbonization Process. *J. Environ. Manage.* **2012**, *109*, 61–  
9 69. DOI: 10.1016/j.jenvman.2012.04.047
- 10 (3) Lodeiro, P.; Herrero, R.; Sastre de Vicente, M. E. Batch Desorption Studies and  
11 Multiple Sorption-regeneration Cycles in a Fixed-bed Column for Cd(II) Elimination by  
12 Protonated *Sargassum muticum*. *J. Hazard. Mater.* **2006**, *137*, 1649–1655. DOI:  
13 10.1016/j.jhazmat.2006.05.003
- 14 (4) Zulfadhly, A.; Mashitah, M. D.; Bhatia, S. Heavy Metals Removal in Fixed-bed  
15 Column by the Macro Fungus *Pycnoporus sanguineus*. *Environ. Pollut.* **2001**, *112*,  
16 463–470. DOI: 10.1016/S0269-7491(00)00136-6
- 17 (5) Beesley, L.; Marmiroli, M. The Immobilisation and Retention of Soluble Arsenic,  
18 Cadmium and Zinc by Biochar. *Environ. Pollut.* **2011**, *159*, 474–480. DOI:  
19 10.1016/j.envpol.2011.07.023
- 20 (6) Xu, X.; Cao, X.; Zhao, L. Comparison of Rice Husk- and Dairy Manure-derived  
21 Biochars for Simultaneously Removing Heavy Metals from Aqueous Solutions: Role of  
22 Mineral Components in Biochars. *Chemosphere* **2013**, *92*, 955–961. DOI:  
23 10.1016/j.chemosphere.2013.03.009

- 1 (7) Bird, M. I.; Wurster, C. M.; Silva, P. H. P.; Bass, A. M.; Nys, R. Algal Biochar –  
2 Production and Properties. *Bioresour. Technol.* **2011**, *102*, 1886–1891. DOI:  
3 10.1016/j.biortech.2010.07.106
- 4 (8) Qiu, Y.; Cheng, H.; Xu, C.; Sheng, G. D. Surface characteristics of crop-residue-  
5 derived black carbon and lead (II) adsorption. *Water Res.* **2008**, *42*, 567–574. DOI:  
6 10.1016/j.watres.2007.07.051
- 7 (9) Arán, D.; Antelo, J.; Fiol, S.; Macías, F. Influence of Feedstock on the Copper  
8 Removal Capacity of Waste-Derived Biochars. *Bioresour. Technol.* **2016**, *212*, 199–  
9 206. DOI: 10.1016/j.biortech.2016.04.043
- 10 (10) Gupta, V. K.; Ali, I.; Saleh, T. A.; Siddiqui, M. N.; Agarwal, S. Chromium  
11 Removal from Water by Activated Carbon Developed from Waste Rubber Tires.  
12 *Environ. Sci. Pollut. Res.* **2013**, *20*, 1261–1268. DOI: 10.1007/s11356-012-0950-9
- 13 (11) Garrido-Rodríguez, B.; Cutillas-Barreiro, L.; Fernández-Calviño, D.; Arias-  
14 Estévez, M.; Fernández-Sanjurjo, M.J.; Álvarez-Rodríguez, E.; Núñez-Delgado, A.  
15 Competitive Adsorption and Transport of Cd, Cu, Ni and Zn in a Mine Soil Amended  
16 with Mussel Shell. *Chemosphere* **2014**, *107*, 379–385. DOI:  
17 10.1016/j.chemosphere.2013.12.097
- 18 (12) Sohi, S.P.; Krull, E.; Lopez-Capel, E.; Bol, R. A Review of Biochar and its Use  
19 and Function in Soil. *Adv. Agron.* **2010**, *105*, 47–82. DOI: 10.1016/S0065-  
20 2113(10)05002-9
- 21 (13) Callery, O.; Healy, M.G.; Rognard, F.; Barthelemy, L.; Brennan, R. B. Evaluating  
22 the Long-Term Performance of Low-Cost Adsorbents Using Small-Scale Adsorption

- 1 Column Experiments. *Water Res.* **2016**, *101*, 429–440. DOI:  
2 10.1016/j.watres.2016.05.093
- 3 (14) Sadaf, S.; Bhatti, H. N. Batch and Fixed Bed Column Studies for the Removal of  
4 Indosol Yellow BG Dye by Peanut Husk. *J. Taiwan Inst. Chem. Eng.* **2014**, *45*, 541–  
5 553. DOI: 10.1016/j.jtice.2013.05.004
- 6 (15) Patrón-Prado, M.; Lodeiro, P.; Lluch-Cota, D. B.; Serviere-Zaragoza, E.; Casas-  
7 Valdez, M.; Zenteno-Savín, T.; Méndez-Rodríguez, L. Efficiency of Copper Removal  
8 by *Sargassum sinicola* in Batch and Continuous Systems. *J Appl. Phycol.* **2013**, *25*,  
9 1933–1937. DOI: 10.1007/s10811-013-0031-6
- 10 (16) Park, J. H.; Cho, J. S.; Ok, Y. S.; Kim, S. H.; Kim, S. H.; Kang, S. W.; Choi, I. W.;  
11 Heo, J. S.; DeLaune, R. D.; Seo, D. C. Competitive Adsorption and Selectivity  
12 Sequence of Heavy Metals by Chicken Bone-Derived Biochar: Batch and Column  
13 Experiment. *J. Environ. Sci. Health, Part A: Toxic/Hazard. Subst. Environ. Eng.* **2015**,  
14 *50*, 1194–1204. DOI: 10.1080/10934529.2015.1047680
- 15 (17) Ramírez-Pérez, A. M.; Paradelo, M.; Nóvoa-Muñoz, J. C.; Arias-Estévez, M.;  
16 Fernández-Sanjurjo, M. J.; Álvarez-Rodríguez, E.; Núñez-Delgado, A. Heavy Metal  
17 Retention in Copper Mine Soil Treated with Mussel Shells: Batch and Column  
18 Experiments. *J. Hazard. Mater.* **2013**, *248-249*, 122–130. DOI:  
19 10.1016/j.jhazmat.2012.12.045
- 20 (18) Chen, J. P.; Yoon, J. T.; Yiaccoumi, S. Effects of Chemical and Physical Properties  
21 of Influent on Copper Sorption onto Activated Carbon Fixed-Bed Columns. *Carbon*  
22 **2003**, *41*, 1635–1644. DOI: 10.1016/S0008-6223(03)00117-9

- 1 (19) Ding, Z.; Hu, X.; Wan, Y.; Wang, S.; Gao, B. Removal of Lead, Copper,  
2 Cadmium, Zinc, and Nickel from Aqueous Solutions by Alkali-Modified Biochar:  
3 Batch and Column Tests. *J. Ind. Eng. Chem.* **2016**, *33*, 239–245. DOI:  
4 10.1016/j.jiec.2015.10.007
- 5 (20) Volesky, B. *Sorption and Biosorption*. BV Sorbex, **2003**
- 6 (21) Business for Social Responsibility, *BSR Water Quality Guidelines*.  
7 [http://www.bsr.org/reports/awqwg/BSR\\_AWQWG\\_Guidelines-Testing-Standards.pdf](http://www.bsr.org/reports/awqwg/BSR_AWQWG_Guidelines-Testing-Standards.pdf).  
8 (accessed May 15, 2017).
- 9 (22) EC, Directive 2010/75/EC of the European Parliament and of the Council - on  
10 Industrial Emissions. *Official Journal European Communities* **2010**, *334*, 17–119.
- 11 (23) BIS IS 2490-1, Tolerance Limits For Industrial Effluents Discharged Into Inland  
12 Surface Waters - Part 1: General Limits. *Bureau of Indian Standard*. **1981**.
- 13 (24) WHO, Copper in drinking water. Background Document for Development of  
14 WHO Guidelines for Drinking-water Quality (WHO/SDE/WSH/03.04/38). *World*  
15 *Health Organization*, Genève. **2004**.
- 16 (25) EC, Directive 98/83/EC of the Council - on the Quality of Water Intended for  
17 Human Consumption. *Official Journal of the European Communities* **1998**, *330*, 32–54.
- 18 (26) US-EPA, Maximum Contaminant Level Goals and National Primary Drinking  
19 Water Regulations for Lead and Copper; Final Rule. *US Environmental Protection*  
20 *Agency. Federal Register*, **1991**, *56*, 26460–26564.

- 1 (27) Yan, G.; Viraraghavan, T.; Chen, M. A New Model for Heavy Metal Removal in a  
2 Biosorption Column. *Adsorpt. Sci. Technol.* **2001**, *19*, 25–43. DOI:  
3 10.1260/0263617011493953
- 4 (28) Chu, K. H. Fixed Bed Sorption: Setting the Record Straight on the Bohart-Adams  
5 and Thomas Models. *J. Hazard. Mater.* **2010**, *177*, 1006–1012. DOI:  
6 10.1016/j.jhazmat.2010.01.019
- 7 (29) Kiran, B.; Kaushik, A. Cyanobacterial Biosorption of Cr(VI): Application of Two  
8 Parameter and Bohart Adams Models for Batch and Column Studies. *Chem. Eng. J.*  
9 **2008**, *144*, 391–399. DOI: 10.1016/j.cej.2008.02.003
- 10 (30) Han, R.; Wang, Y.; Zhao, X.; Wang, Y.; Xie, F.; Cheng, J.; Tang, M. Adsorption  
11 of Methylene Blue by Phoenix Tree Leaf Powder in a Fixed-Bed Column: Experiments  
12 and Prediction of Breakthrough Curves. *Desalination* **2009**, *245*, 284–297. DOI:  
13 10.1016/j.desal.2008.07.013
- 14 (31) Ahmad, M.; Rajapaksha, A. U.; Lim, J. E.; Zhang, M.; Bolan, N.; Mohan, D.;  
15 Vithanage, M.; Lee, S. S.; Ok, Y. S. Biochar as a Sorbent for Contaminant Management  
16 in Soil and Water: A Review. *Chemosphere* **2014**, *99*, 19–33. DOI:  
17 10.1016/j.chemosphere.2013.10.071
- 18 (32) Xiao, X.; Chen, Z.; Chen, B. H/C atomic ratio as a smart linkage between pyrolytic  
19 temperatures, aromatic clusters and sorption properties of biochars derived from diverse  
20 precursory materials. *Scientific Reports* **2016**, *6*, 22644. DOI:10.1038/srep22644.
- 21 (33) Ahmad, M.; Lee, S. S.; Dou, X.; Mohan, D.; Sung, J.; Yang, J. E.; Ok, Y. S. Effects of  
22 Pyrolysis Temperature on Soybean Stover- and Peanut Shell- Derived Biochar  
23 Properties and TCE Adsorption in Water. *Bioresour. Technol.* **2012**, *118*, 536–544.

- 1 DOI: 10.1016/j.biortech.2012.05.042
- 2 (34) Chen, X.; Chen, G.; Chen, L.; Chen, Y.; Lehmann, J.; McBride, M. B.; Hay, A. G.  
3 Adsorption of Copper and Zinc by Biochars Produced from Pyrolysis of Hardwood and  
4 Corn Straw in Aqueous Solution. *Bioresour. Technol.* **2011**, *102*, 8877–8884. DOI:  
5 10.1016/j.biortech.2011.06.078
- 6 (35) Chen, B.; Zhou, D.; Zhu, L. Transitional Adsorption and Partition of Nonpolar and  
7 Polar Aromatic Contaminants by Biochars of Pine Needles with Different Pyrolytic  
8 Temperatures. *Environ. Sci. Technol.* **2008**, *42*, 5137–5143. DOI: 10.1021/es8002684
- 9 (36) Chun, Y.; Sheng, G.; Chiou, C. T.; Xing, B. Compositions and Sorptive Properties  
10 of Crop Residue-Derived Chars. *Environ. Sci. Technol.* **2004**, *38*, 4649–4655. DOI:  
11 10.1021/es035034w
- 12 (37) Sağ, Y.; Nourbakhsh, M.; Aksu, Z.; Kutsal, T. Comparison of Ca-alginate and  
13 Immobilized *Z. ramigera* as Sorbents for Copper (II) Removal. *Process Biochem.* **1995**,  
14 *30*, 175–181. DOI: 10.1016/0032-9592(95)80009-3
- 15 (38) Ahmad, A. A.; Hameed, B. H. Fixed-bed Adsorption of Reactive Azo Dye onto  
16 Granular Activated Carbon Prepared from Waste. *J. Hazard. Mater.* **2010**, *175*, 298–  
17 303. DOI: 10.1016/j.jhazmat.2009.10.003
- 18 (39) Gustafsson, J.P. Visual MINTEQ, version 3.1. Department of Land and Water  
19 Resources Engineering, KTH, Stockholm, Sweden, **2014**.
- 20 (40) Xu, X.; Zhao, Y.; Sima, J.; Zhao, L.; Masek, O.; Cao, X. Indispensable Role of  
21 Biochar-inherent Mineral Constituents in its Environmental Applications: A Review.  
22 *Bioresour. Technol.* **2017**, *241*, 887-899. DOI: 10.1016/j.biortech.2017.06.023



- 1 (41) Uchimiya, M.; Lima, I. M.; Klasson, K. T.; Chang, S. C.; Wartelle, L. H.; Rodgers,  
2 J. E. Immobilization of Heavy Metal Ions (Cu-II, Cd-II, Ni-II, and Pb-II) by Broiler  
3 Litter-derived Biochars in Water and Soil. *J. Agric. Food Chem.* **2010**, *58*, 5538–5544.  
4 DOI: 10.1021/jf9044217
- 5 (42) Peng, H.; Gao, P.; Chu, G.; Pan, B.; Peng, J.; Xing, B. Enhanced adsorption of  
6 Cu(II) and Cd(II) by phosphoric acid-modified biochars. *Environ. Pollut.* **2017**, *229*,  
7 846–853. DOI:10.1016/j.envpol.2017.07.004
- 8 (43) Kuo, S. Phosphorus, in Spark D.K.; Page, A.L.; Helmke, P.A.; Loeppert, R.H.;  
9 Soltanour, P.N.; Tabatabai, M.A.; Johnston, C.T.; Sumner, M.E. (Eds.) *Methods of Soil*  
10 *analysis. Part 3. Chemical Methods*. SSSA, Madison, Wisconsin, **1996**.
- 11 (44) Komkiene, J.; Baltreinaite, E. Biochar as Adsorbent for Removal of Heavy Metal  
12 Ions [Cadmium(II), Copper(II), Lead(II), Zinc(II)] from Aqueous Phase. *Int. J. Environ.*  
13 *Sci. Technol.* **2016**, *13*, 471–482. DOI: 10.1007/s13762-015-0873-3
- 14 (45) Muhamad, H.; Doan, H.; Lohi, A. Batch and Continuous Fixed-bed Column  
15 Biosorption of Cd<sup>2+</sup> and Cu<sup>2+</sup>. *Chem. Eng. J.* **2010**, *158*, 369–377.  
16 DOI:10.1016/j.cej.2009.12.042
- 17 (46) Ghaedi, A. M.; Ghaedi, M.; Vafaei, A.; Iravani, N.; Keshavarz, M.; Rada, M.;  
18 Tyagi, I.; Agarwal, S.; Gupta, V. K. Adsorption of Copper (II) Using Modified  
19 Activated Carbon Prepared from Pomegranate Wood: Optimization by Bee Algorithm  
20 and Response Surface Methodology. *J. Mol. Liq.* **2015**, *206*, 195–206. DOI:  
21 10.1016/j.molliq.2015.02.029
- 22 (47) Alslaiibi, T. M.; Abustan, I.; Azmier, M.; Foul, A. A. Kinetics and Equilibrium  
23 Adsorption of Iron (II), Lead (II), and Copper (II) onto Activated Carbon Prepared from

1 Olive Stone Waste. *Desalin. Water Treat.* **2014**, *52*, 7887–7897. DOI:  
2 10.1080/19443994.2013.833875

3 (48) Meng, J.; Wang, L.; Liu, X.; Wu, J.; Brooks, P. C.; Xu, J. Physicochemical  
4 properties of biochar produced from aerobically composted swine manure and its  
5 potential use as an environmental amendment. *Bioresour. Technol.* **2013**, *142*, 641–646.  
6 DOI:10.1016/j.biortech.2013.05.086

7

1 **Figure captions**

2 Figure 1. Experimental set-up of adsorption columns

3 Figure 2. Breakthrough curves for Cu removal by CCBC at different flow rates. The  
4 symbols represent the average of two independent experimental replicates. The error  
5 bars represent the standard deviation of the experimental replicates. The lines represent  
6 the modified Bohart-Adams model fit

7 Figure 3. Variation in breakthrough,  $t_b$ , and exhaustion,  $t_e$ , times in relation to the flow  
8 rate

9 Figure 4. Breakthrough curves for Cu removal by different types of BC at a constant  
10 flow rate  $7 \text{ mL min}^{-1}$ . The symbols represent the average of two independent  
11 experimental replicates. The error bars represent the standard deviation of the  
12 experimental replicates. The lines represent the modified Bohart-Adams model fit

13 Figure 5. Correlation between the maximum retention capacities predicted by the  
14 empirical models for batch and continuous flow experiments.  $Q_{max}$  values obtained with  
15 the Lagmuir-Freundlich model are taken from Arán et al.<sup>9</sup>

16

17

18

19

1 **Table captions**

2 Table 1. Physicochemical characteristics of the different types of biochar

3 Table 2. Parameters obtained from the breakthrough curves of copper adsorption by  
4 CCBC at different flow rates

5 Table 3. Parameters obtained from the non-linear fit of the modified Bohart-Adams  
6 model to the breakthrough curve for CCBC

7 Table 4. Parameters obtained from the breakthrough curves of copper adsorption by  
8 different types of BC at a constant flow rate of  $7.0 \text{ mL min}^{-1}$

9 Table 5. Parameters obtained by fitting the modified Bohart-Adams model to the  
10 breakthrough curves for the different BCs

11

1 **Table 1.** Physicochemical characteristics of the different types of biochar.

	OBC	CMBC	SBC	EBC	CCBC
pH	9.57	7.15	4.94	5.19	10.10
%C	31.1	32.6	62.6	69.3	85.2
%N	2.10	3.02	0.67	0.41	0.80
%H	2.40	3.90	3.67	5.10	2.10
%S	0.08	0.32	0.04	0.01	0.10
%Ash	49.5	46.4	2.13	1.90	3.90
%O	14.8	13.7	30.8	23.2	7.90
O/C	0.35	0.32	0.37	0.25	0.07
H/C	0.94	1.45	0.70	0.88	0.29
S <sub>BET</sub> (m <sup>2</sup> g <sup>-1</sup> )	3.80	1.79	43.28	1.60	173.0
P (g kg <sup>-1</sup> )	3.29	15.30	0.24	0.21	0.86

2

3

1 **Table 2.** Parameters obtained from the breakthrough curves of copper adsorption by  
2 CCBC at different flow rates.

<b>Flow (mL min<sup>-1</sup>)</b>	<b>13.0</b>	<b>7.0</b>	<b>5.0</b>	<b>2.5</b>
<b>q<sub>t</sub> (mg)</b>	32.16	32.14	24.46	18.22
<b>q<sub>e</sub> (mg g<sup>-1</sup>)</b>	6.43	6.64	4.89	3.64
<b>t<sub>b</sub> (h)</b>	3.08	5.17	11.66	18.25
<b>t<sub>e</sub> (h)</b>	19.54	24.0	31.00	39.63
<b>Z<sub>m</sub> (cm)</b>	7.58	7.06	5.61	4.83
<b>Δt (h)</b>	15.96	18.83	20.00	21.38

3

4

1 **Table 3.** Parameters obtained from the non-linear fit of the modified Bohart-Adams  
2 model to the breakthrough curve for CCBC.

<b>Flow rate (mL min<sup>-1</sup>)</b>	<b>q<sub>max</sub> (mg g<sup>-1</sup>)</b>	<b>a</b>	<b>R<sup>2</sup></b>	<b>RRS</b>
<b>13</b>	5.51 ± 0.06	3.2 ± 0.1	0.995	0.023
<b>7.0</b>	3.78 ± 0.03	4.6 ± 0.2	0.992	0.036
<b>5.0</b>	4.55 ± 0.06	5.6 ± 0.3	0.988	0.045
<b>2.5</b>	3.48 ± 0.04	6.7 ± 0.4	0.984	0.102

3

4

5

1 **Table 4.** Parameters obtained from the breakthrough curves of copper adsorption by  
 2 different types of BC at a constant flow rate of 7.0 mL min<sup>-1</sup>.

Type of BC	CMBC	OBC	EBC	CCBC	SBC
<b>q<sub>total</sub> (mg)</b>	136.98	124.35	26.79	32.14	14.87
<b>q<sub>e</sub> (mg g<sup>-1</sup>)</b>	27.40	24.87	5.36	6.64	2.97
<b>t<sub>b</sub> (h)</b>	47.00	47.25	9.50	5.17	0.25
<b>t<sub>e</sub> (h)</b>	86.00	82.00	25.30	24.0	16.00
<b>Z<sub>m</sub> (cm)</b>	4.08	3.81	5.62	7.06	8.86
<b>Δt (h)</b>	39.00	34.75	15.80	18.83	17.75

3

4



1 **Table 5.** Parameters obtained by fitting the modified Bohart-Adams model to the  
2 breakthrough curves for the different BCs.

	$q_{\max}$ (mg g <sup>-1</sup> )	a	R <sup>2</sup>	RRSE
<b>CMBC</b>	26.6 ± 0.26	6.43 ± 0.46	0.978	0.042
<b>OBC</b>	25.3 ± 0.11	9.12 ± 0.36	0.992	0.022
<b>EBC</b>	5.28 ± 0.08	6.40 ± 0.52	0.978	0.008
<b>CCBC</b>	3.78 ± 0.03	4.62 ± 0.19	0.992	0.036
<b>SBC</b>	1.28 ± 0.07	0.66 ± 0.03	0.980	0.007

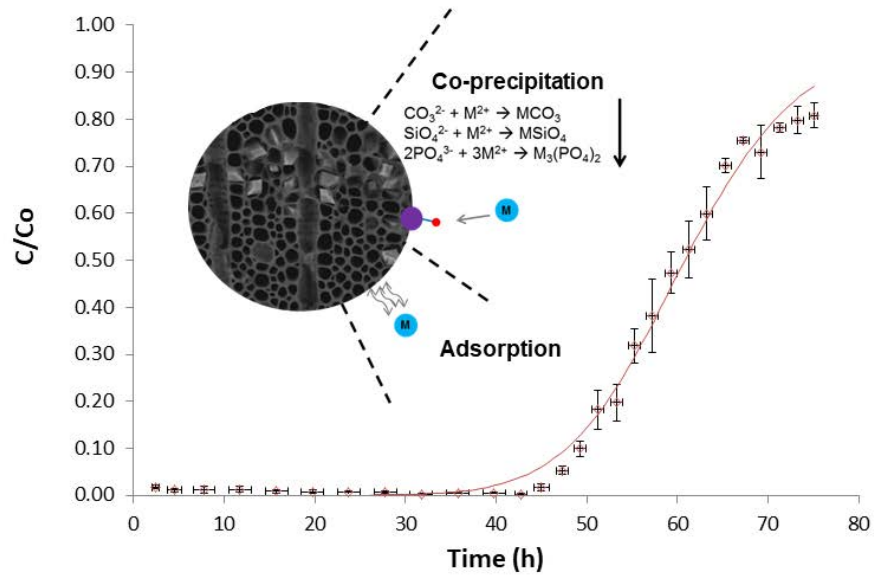
3

4

5

# 1 Graphical Abstract

2

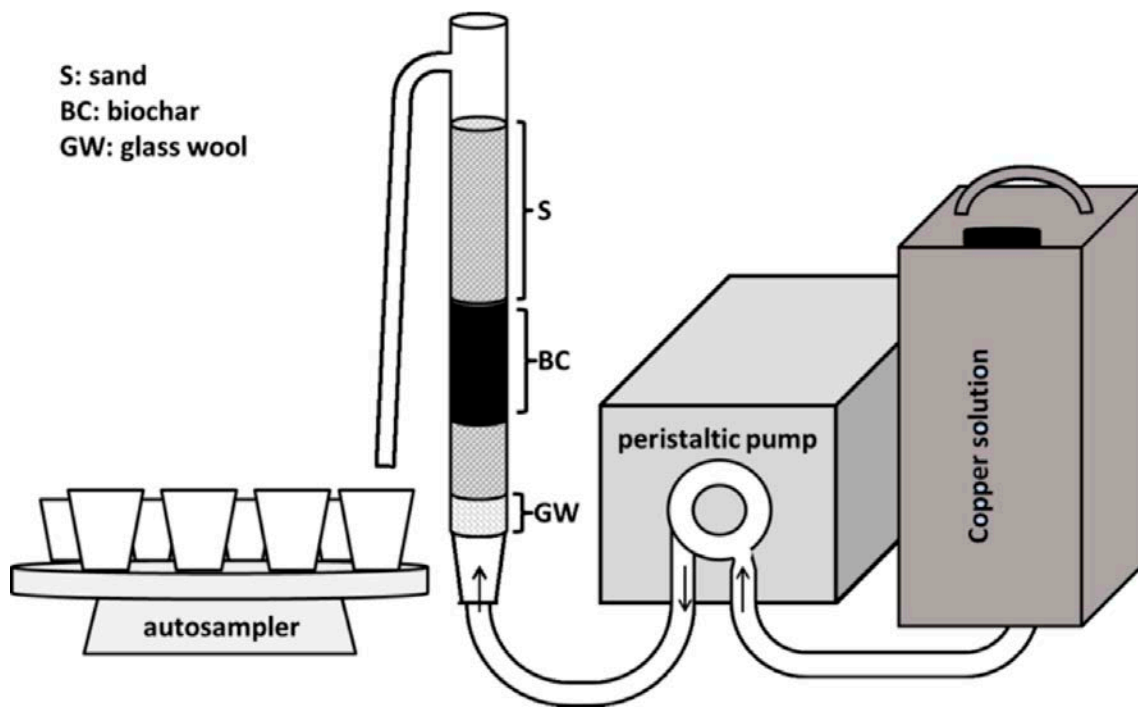


3

4

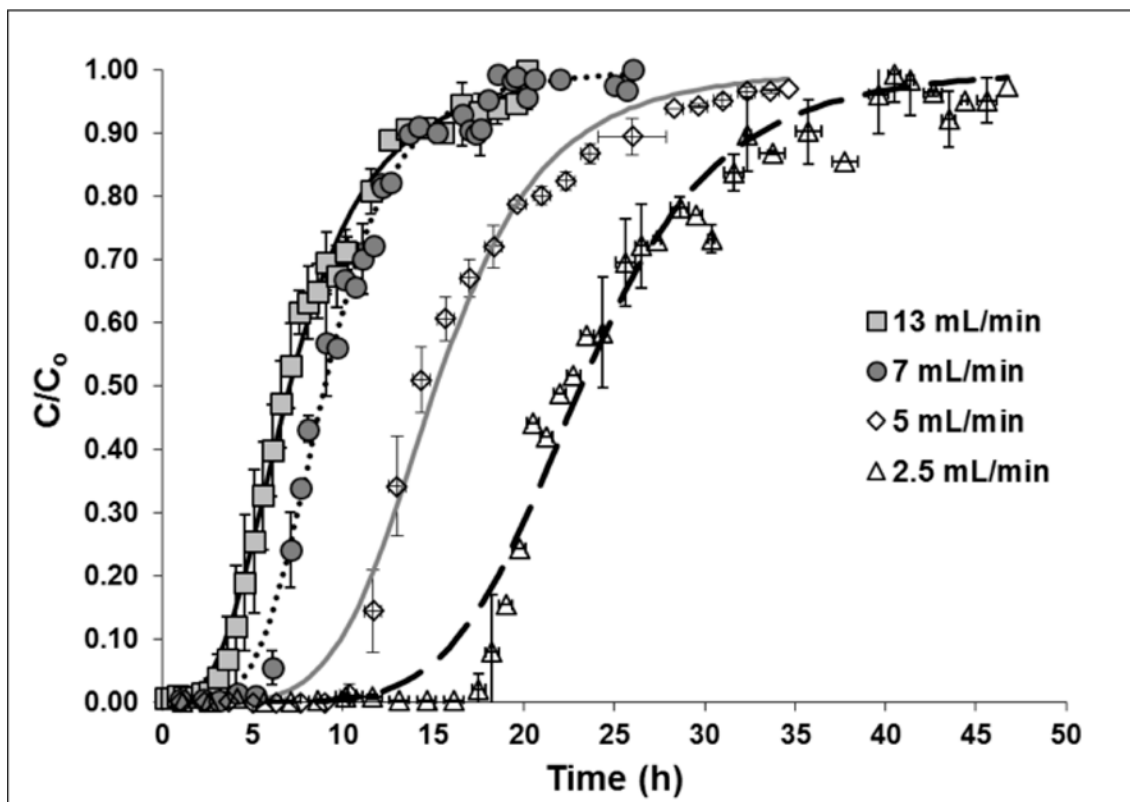
5

1 **Figure 1.** Experimental set-up of adsorption columns



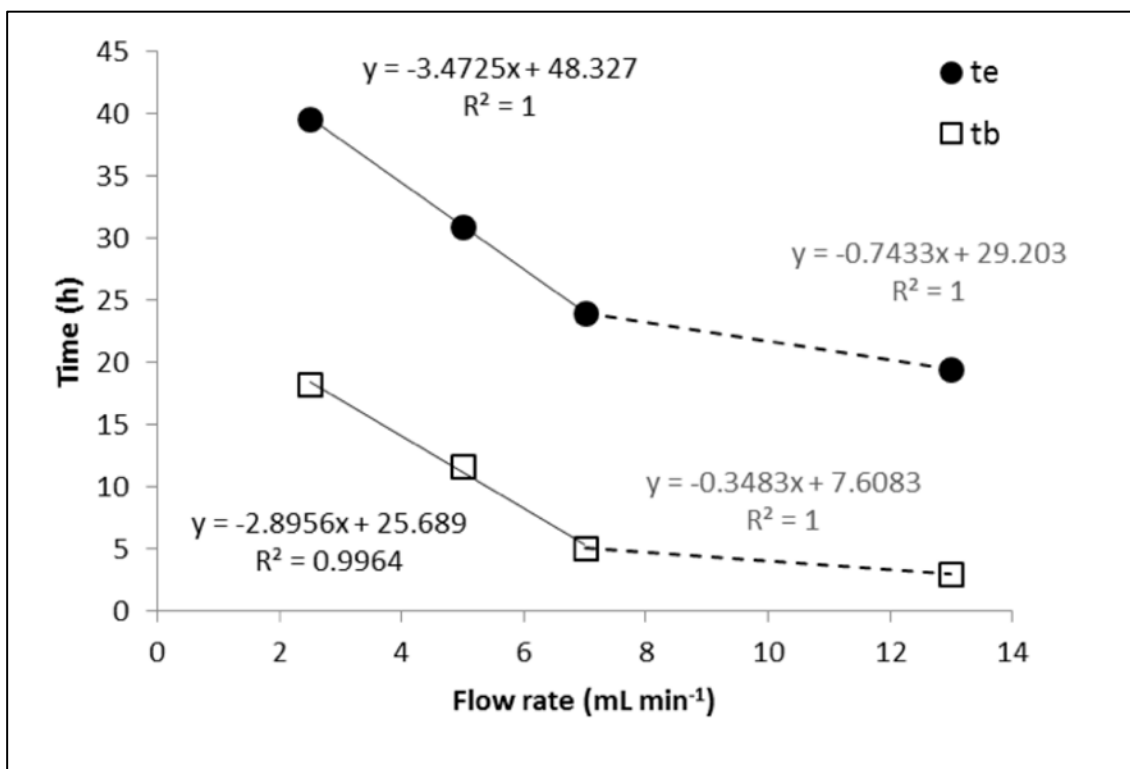
2  
3

1 **Figure 2.** Breakthrough curves for Cu removal by CCBC at different flow rates. The  
2 symbols represent the average of two independent experimental replicates. The error  
3 bars represent the standard deviation of the experimental replicates. The lines represent  
4 the modified Bohart-Adams model fit



5  
6  
7

1 **Figure 3.** Variation in breakthrough,  $t_b$ , and exhaustion,  $t_e$ , times in relation to the flow  
2 rate

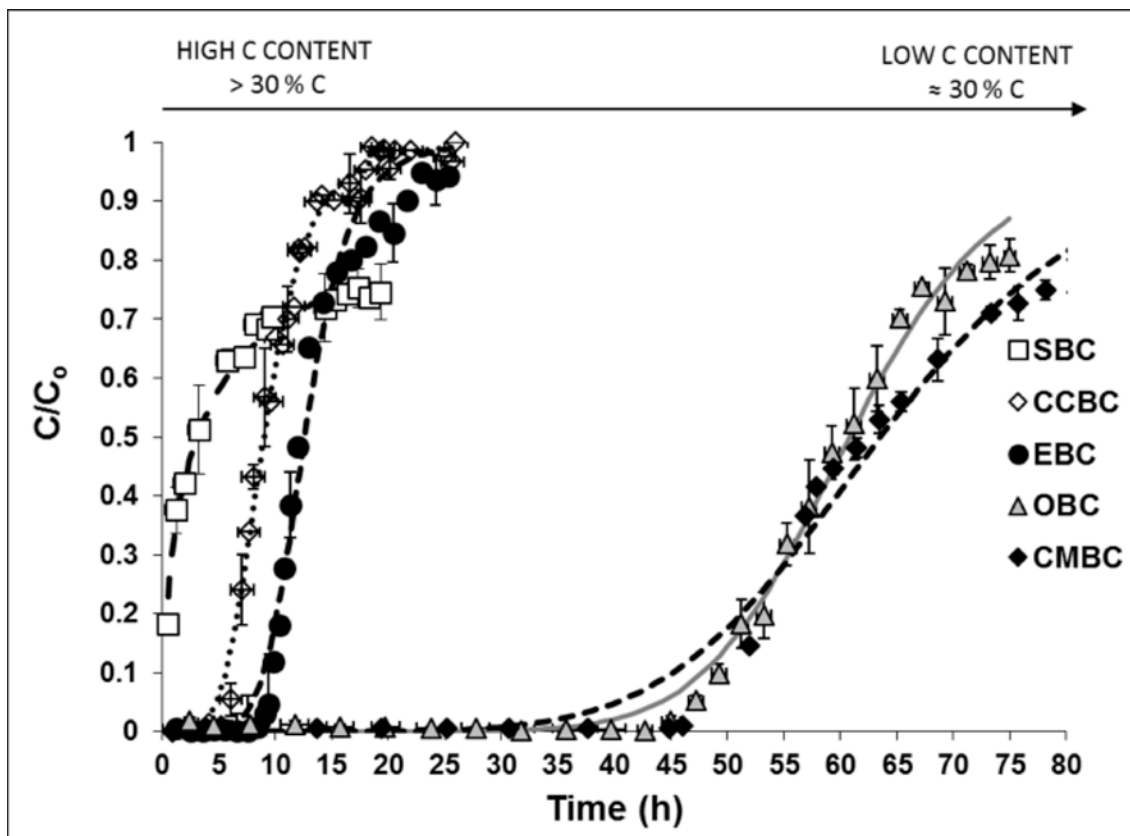


3

4

5

1 **Figure 4.** Breakthrough curves for Cu removal by different types of BC at a constant  
2 flow rate  $7 \text{ mL min}^{-1}$ . The symbols represent the average of two independent  
3 experimental replicates. The error bars represent the standard deviation of the  
4 experimental replicates. The lines represent the modified Bohart-Adams model fit

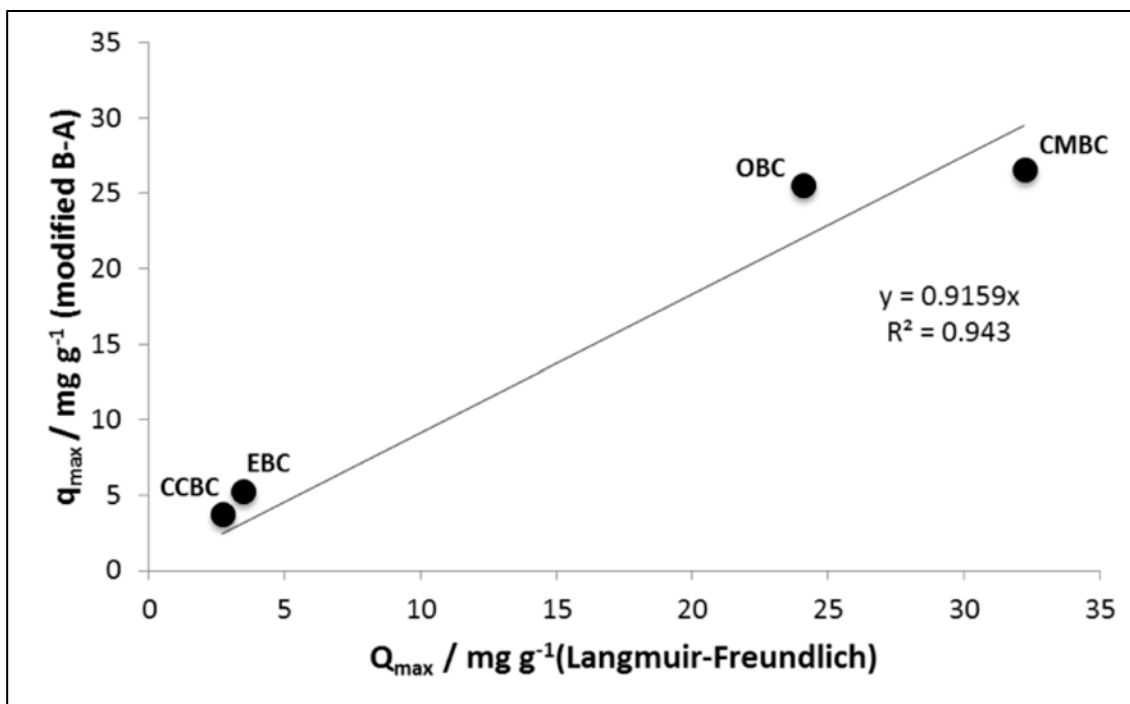


5

6

7

1 **Figure 5.** Correlation between the maximum retention capacities predicted by the  
2 empirical models for batch and continuous flow experiments.  $Q_{max}$  values obtained with  
3 the Lagmuir-Freundlich model are taken from Arán et al.<sup>9</sup>



4

5